IEEE Open Journal of
Power Electronics

Received 6 March 2024; revised 1 April 2024; accepted 7 April 2024. Date of publication 10 April 2024;
date of current version 24 April 2024. The review of this paper was arranged by Associate Editor Cong Li.

Digital Object Identifier 10.1109/OJPEL.2024.3387076

β-Ga_2O_3 in Power Electronics Converters: Opportunities & Challenges

SAEED JAHDI [1] (Senior Member, IEEE), AKHIL S. KUMAR [2] (Member, IEEE), MATTHEW DEAKIN [3] (Member, IEEE), PHIL C. TAYLOR [1] (Senior Member, IEEE), AND MARTIN KUBALL [2] (Fellow, IEEE)

[1]Electrical Energy Management Group, Department of Electrical Engineering, University of Bristol, BS8 1UB Bristol, U.K.
[2]Center for Device Thermography and Reliability (CDTR) of School of Physics, University of Bristol, BS8 1TL Bristol, U.K.
[3]Electrical Power group in the School of Engineering, Newcastle University, NE1 7RU Newcastle upon Tyne, U.K.

CORRESPONDING AUTHOR: SAEED JAHDI (e-mail: saeed.jahdi@bristol.ac.uk)

The work of Saeed Jahdi was supported by U.K. Royal Society Research under Grant RGS/R2/202193. The work of Matthew Deakin was supported by the U.K. Royal Academy of Engineering under the Research Fellowship Programme. The work of Martin Kuball was supported by the Royal Academy of Engineering through Chair in Emerging Technologies scheme. This work was supported in part by U.K. Engineering and Physical Research Council as Supergen Energy Networks Hub under Grant EP/S00078X/2, in part by ULTRA, an Energy Frontier Research Center funded by the U.S. Department of Energy, Office of Science, Basic Energy Sciences at the University of Bristol under Award DE-SC0021230.

ABSTRACT In this work, the possibility of using different generations of β-Ga_2O_3 as an ultra-wide-bandgap power semiconductor device for high power converter applications is explored. The competitiveness of β-Ga_2O_3 for power converters in still not well quantified, for which the major determining factors are the on-state resistance, R_{ON}, reverse blocking voltage, V_{BR}, and the thermal resistance, R_{th}. We have used the best reported device specifications from literature, both in terms of reports of experimental measurements and potential demonstrated by computer-aided designs, to study power converter performance for different device generations. Modular multilevel converter-based voltage source converters are identified as a topology with significant potential to exploit these device characteristics. The performance of MVDC & HVDC converters based on this topology have been analysed, focusing on system level power losses and case temperature rise at the device level. Comparisons of these β-Ga_2O_3 devices are made against contemporary SiC-FET and Si-IGBTs. The results have indicated that although the early β-Ga_2O_3 devices are not competitive to incumbent Si-IGBT and SiC-FET modules, the latest experimental measurements on NiO_X/β-Ga_2O_3 and β-Ga_2O_3/diamond significantly surpass the performance of incumbent modules. Furthermore, parameters derived from semiconductor-level simulations indicate that the β-Ga_2O_3/diamond in superjunction structures delivers even superior performance in these power converters.

INDEX TERMS β-Ga_2O_3, diamond, gallium oxide, HVDC converters, ultra-wide-bandgap.

I. INTRODUCTION

Strategies to achieve net-zero carbon emissions are urgently required to arrest global warming and ensure a sustainable economy for future generations. A leading framework that has been proposed for this net-zero transition is electrification – i.e., first pursue power sector decarbonisation, then aggressively convert other carbon-intensive sectors to be powered from the clean power sector (either directly, or through multi-vector energy transfers). Power electronics are a crucial technology for this approach, as they are central for many power generation, distribution, storage, multi-vector conversion, and end-use approaches. Unfortunately, converters suffer a number of drawbacks as compared to legacy power system technologies, often having higher costs, higher losses, lower reliability, more complicated control, and lack the inherent inertia of electrical machines. Given these issues, and the urgency of the net zero transition, it is imperative that the most promising technologies for increasing converter performance are investigated thoroughly. As a core component of all power converters, the development of new devices

using novel semiconductor materials has a particular significance for addressing shortcomings of power electronics, with potential to achieve impact across the energy sector globally.

The success of Si-based power semiconductors was chiefly driven by its cost effectiveness owing to melt-grown substrate. Enhancement of operating voltage close to 2 kV has been possible using Si-Insulated Gate Bipolar Transistor (Si-IGBT) [1]. It has been envisioned that future needs of increased operation voltage can be achieved by migrating to SiC and GaN [2], [3], [4], [5], [6], [7]. However, the cost advantage could be lost as e.g. SiC is simply more expensive. Again, the usability of these technologies for ultrahigh-power applications ($>$ 20 kV) is not well studied. In such a scenario, an alternative semiconductor technology offering both very high operating voltage capabilities along with its low-cost benefits would be the ideal candidate to help decarbonize the power sector.

The Figure of Merit (FoM) derived by Baliga (BFOM) is widely used as a metric for the selection of semiconductor materials for power switching applications [8]. Although BFOM is suitable at the material level, it deviates due to increasing complexity of losses involved and thermal management ability at the device level. To the first order, BFOM is proportional to $\varepsilon\mu E_C^3$, where ε is the dielectric constant, μ is the mobility and E_C is the critical electric field of a material. The cubic power law dependence of E_C on bandgap (E_G) makes ultra-wide bandgap (UWBG) semiconductors lucrative for high power applications. Although there are few contenders for UWBG materials like Aluminium Nitride, Boron Nitride, and diamond, there is an increasing interest in the research community on β-Ga_2O_3, as similar to Si, melt-grown low-cost substrates are possible, commercially available up to 4 in, and have been demonstrated even up to 6 in.

In this work, the opportunities and challenges of the implementation of β-Ga_2O_3 devices in heavy-duty power electronics applications is discussed. Different generations of β-Ga_2O_3 are considered, including the results of reports of experimental measurements on β-Ga_2O_3, NiO_X/β-Ga_2O_3 and β-Ga_2O_3/diamond to theoretical designs of the potentials of these devices in applications, e.g., when fabricated in superjunction structures. In Section II, the improvement in performance of β-Ga_2O_3-based diodes is presented where a first-order analysis, ignoring switching loss and thermal conductivity, is presented. Section III summarizes converter topologies where these devices can make a difference. This section invokes a realistic approach of switching losses and thermal conductivity at the device level; Section IV shows results of simulations in the testbed of MVDC & HVDC converters, while Section V concludes the work.

II. STATE-OF-THE-ART ULTRA-WIDE-BANDGAP DEVICES

At the device level, BFOM can be reduced to V_{BR}^2/R_{ON}, where V_{BR} is the device breakdown voltage and R_{ON} is the on-resistance in Ω-mm^2. The β-Ga_2O_3 with an E_G close to 4.8 eV is expected to produce an E_C of 8 MV/cm [9]. This would result in a theoretical BFOM of approximately 40 GW/cm^2 for β-Ga_2O_3 assuming mobility in the range of 250-300 cm^2/V.s. This value is approximately 4x and 10x higher than that of GaN and SiC, respectively [9]. This places β-Ga_2O_3 as the preferred candidate for ultrahigh voltage power applications. Another crucial factor determining market penetration is the cost of wafer. The β-Ga_2O_3 substrate is melt-grown similar to Si, which provides additional cost advantage e.g. over the SiC with its vapour phase grown substrates [10].

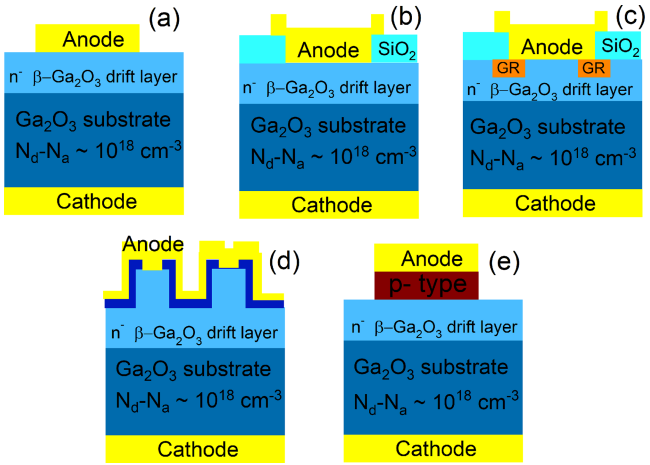

FIGURE 1. Structural evolutions of β-Ga_2O_3 diodes which have resulted in improved figures of merit.

Since the first report of electric field effect action in β-Ga_2O_3 in 2012, various research groups have come up with novel device designs to improve the performance of β-Ga_2O_3 diodes and transistors [11]. The evolution of β-Ga_2O_3 diode structure from SBD to latest heterojunction-based diode is shown in Fig. 1. The early developments on vertical β-Ga_2O_3 diodes have shown low R_{ON} simultaneously with high V_{BR}. Conventional Schottky Barrier Diodes (SBD), as shown in Fig. 1(a), with an epitaxial grown drift layer having N $_d$-N_a of 10^{16}-10^{17} cm$_{-3}$ resulted in V_{BR} up to 500 V with R_{ON} of 3 Ω-cm^2 [12]. Other device architectures like field plates in Fig. 1(b) and ion-implanted guard rings in Fig. 1(c) further helped achieve V_{BR} greater than 1 kV [13], [14]. Tri-gated fin based vertical diodes in Fig. 1(d) could increase the V_{BR} to 2 kV but come at the cost of an increased R_{ON} (10 Ω-cm^2) [15], [16]. P-N junction-based diodes are known to have higher breakdown compared to Schottky diodes. However, the development of β-Ga_2O_3 based homojunction p-n diodes is hampered by the challenge achieving p-doping of β-Ga_2O_3 [9]. This led to the exploration of heterojunction P-N diode using p-doped Cu_2 O and NiO $_X$ [17], [18] in Fig. 1(e). Such heterojunction P-N diodes have resulted in diode performance superior to pure β-Ga_2O_3 based SBD. Recent data shows the performance NiO_X/β-Ga_2O_3 diodes exceeding that of the theoretical limit of SiC, and fast approaching towards the GaN limit [19]. This high performance was achieved by the optimization of thickness and doping of the drift region and exploiting the benefits of integrating p-type NiO_X into the

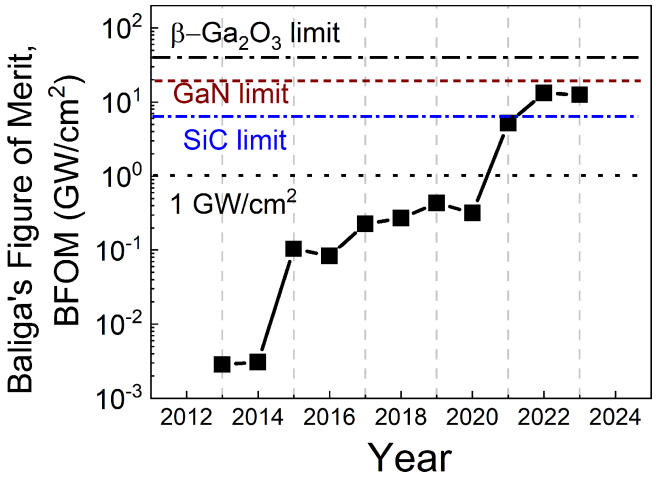

FIGURE 2. Progression in the performance improvement of β-Ga_2O_3-based diodes with year.

β-Ga_2O_3 devices. A drift layer with doping 5-7x10^{15} cm−3 and thickness of 13 μ m was able to achieve V_{BR} of 8.32 kV and R_{ON} of 5.24 Ω-cm^2, resulting in the record high BFOM of 13.2 GW/cm^2. Similar P-N diodes with high performance have also been found to be reproducible by other groups [20]. Large area diodes based on these techniques have demonstrated > 100 A of current and up to 2 kV of breakdown [21]. In Fig. 2, the progression of BFOM for β-Ga_2O_3 diodes is plotted with year. A comparison has also been made with the theoretical limit of SiC and GaN. This clearly shows that recent β-Ga_2O_3 diodes exceed the electrical performance of SiC and is fast approaching the theoretical limit of GaN. This also shows that there is scope for further improving the performance of β-Ga_2O_3 diodes.

All these improvements have been achieved despite the poor thermal conductivity of β-Ga_2O_3 (0.2 W/cm.K), which is 8x smaller than that of GaN and 30x smaller than SiC [9]. Poor thermal conductivity of the material has been known to degrade the ON-state operation of β-Ga_2O_3 transistors, and will impact switching when high voltage and high current is present, potentially impacting also device reliability. Although this low thermal conductivity would severely limit β-Ga_2O_3 in its utility for high power RF electronics compared to power electronics; there is still some interest in the community. For example, current droop in these devices has been established to be the result of self-heating arising from poor thermal management [22]. Trapping effects in conjunction with self-heating has been found to further degrade the high-power performance in these transistors [23]. Additional traps are found to be generated during OFF state stress of β-Ga_2O_3 devices, power or RF devices [24]. This could potentially worsen the self-heating effects in ON state for uses of β-Ga_2O_3 in power devices. Owing to the smaller R_{ON} in β-Ga_2O_3 compared to SiC, its device footprint is expected to be smaller, which calls for novel heat extraction at the device level. Thus, efficient heat management techniques will be the next vital step in device improvements of β-Ga_2O_3 towards the goal of reaching its theoretical limit.

Various strategies have been employed to dissipate the heat in β-Ga_2O_3 at both package and device level. Although packaging of β-Ga_2O_3 devices has shown reduction in thermal resistance, it introduces additional device footprint, undesirable parasitic components and thermo-mechanical stress [25]. Alternatively, integration of diamond with the β-Ga_2O_3 is being vigorously pursued by the research community for the purpose of improved heat extraction at the device level. This is facilitated by the high thermal conductivity of diamond (> 20 W/cm.K). Thin films of β-Ga_2O_3 on diamond have shown promising thermal boundary conductance [26]. Direct bonded diamond as substrate with thin exfoliated β-Ga_2O_3 has exhibited atomistic bonding without void and the device's performance was better than conventional SBD [27]. Electro-thermal studies using diamond as heat spreader in the active region along with the diamond substrate has been found to result in lower transient and steady-state temperature in β-Ga_2O_3 lateral devices by 64% [28]. Electrical and thermal simulations of diamond-Al $_2$ O_3-Ga $_2$ O_3 based superjunction Schottky diodes have shown potential for V_{BR} > 4 kV with R_{ON} of 1-3 Ω-cm^2, at 60% lower operating temperature [29].

In this work, we have explored the possibility of using the different generations of β-Ga_2O_3 materials/devices for ultra-high power converter applications. The competitiveness of β-Ga_2O_3 for power converters is not quantified on a converter level, for which the major determining factors are the on-state resistance, R_{ON}, blocking voltage, V_{BR}, switching loss, and the thermal resistance, R_{th}. Another crucial parameter determining the competitiveness of any semiconductor technology is the cost-performance trade-off. To estimate the cost benefits of different technologies, techno-economic factors like cost of wafer, fabrication, areal density, dicing and packaging needs to be invoked. Accurate modelling exercise has found that the dominant factor determining the cost is that of the wafer which us roughly 60–70 percentage of the overall cost [30]. Cost analysis on 6-inch wafers using techno-economic factors has found the cost of β-Ga_2O_3 to be one-third that of SiC. When compared with Si, the cost of β-Ga_2O_3 wafer is found to be almost the same due to both employing melt-grown technique for wafer growth. Adoption of innovation growth techniques are expected to further reduce the cost of β-Ga_2O_3. However, the integration of diamond into β-Ga_2O_3, mentioned in this work, could increase the overall cost. This study is still in the research phase or has not yet been implemented. The lack of any specific area of application renders the cost-performance analysis premature at this stage. We have used the best reported device specifications from literature and performed circuit and system level simulations. Comparisons have been done with the contemporary SiC-FET and Si-IGBTs.

III. OPPORTUNITIES FOR UWBG DEVICES IN ENERGY SYSTEMS APPLICATIONS

For power converters used in utility applications, the attractive physical properties of β-Ga_2O_3 can translate to three main

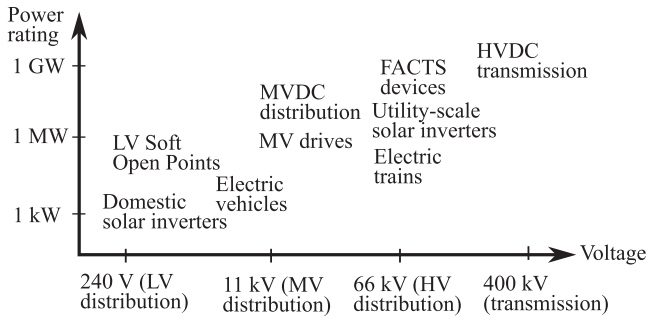

FIGURE 3. Applications of power converters in power systems for power transmission, distribution, and usage.

potential benefits: reduced cost of semiconductor devices, due to simplified manufacturing processes and lower substrate cost; increased efficiency and reduced losses, due to lower R_{ON}; and increased V_{BR} for a given device layer thickness, due to the increased semiconductor bandgap. If these theoretical benefits can be realized in actual devices that become commercially available, there is potential for widespread market adoption, if improved converter performance can be demonstrated. Firstly, if the upfront cost for devices of a given power rating are lower, this immediately makes β-Ga_2O_3 more attractive. Increased efficiency reduces lifetime running costs, and reduces the total energy that must be dissipated by a converter's thermal management system (albeit with the novel device-level thermal management innovations required for β-Ga_2O_3 described in Section II). This leads to overall lower costs required for the converter's cooling system. Finally, higher voltage devices enable greater flexibility in the selection of converter topologies for a given power or voltage rating.

We consider here topologies and technologies which could take advantage of these benefits to consider the most promising applications of β-Ga_2O_3 in the power and energy sector. Particularly, our goal is to identify technologies for which superior efficiency and high voltage devices can be most beneficial. Modular-Multilevel-Converter Voltage-Sourced-Converters (MMC-VSC)-based technologies, used in DC transmission systems, are identified as one application for which β-Ga_2O_3 is considered to have significant potential. The main requirements of utility-scale VSC systems and the impacts of β-Ga_2O_3 on these MMC converters are then covered, highlighting how a reduced number of submodules and increased efficiency could improve performance.

A. CONVERTERS FOR POWER SYSTEM APPLICATIONS: EXISTING AND EMERGING USE-CASES

The use-cases of power converters can be split according to their power and voltage rating, and a non-exhaustive list of applications is presented in Fig. 3. At low voltage (LV) distribution voltage ratings (less than 1 kV), a range of topologies can be exploited with silicon MOSFET or IGBT devices. For example, using Si devices, solar inverters for single phase 230 V European grids can be designed with or without galvanic isolation, using either high-frequency or grid-frequency transformers, and with single- or multi-stage active conversion stages [31]. In these cases, cost is the main concern, with power density and efficiency less critical for most consumers. Nevertheless, at these relatively low converter system ratings, WBG devices are sometimes used in specialist applications where high-power density, efficiency, or frequency switching is required. In the context of automotive applications, for example, the Tesla Model 3 uses SiC to improve efficiency [32], increasing range for electric vehicles (EV) and reducing requirements for thermal management. Silicon IGBTs used for LV 'soft open points' were found to have unacceptable levels of audible noise [33], and so those converters have more recently been built using SiC MOSFETs utilizing higher switching frequencies [34]. In these LV applications, β-Ga_2O_3 could be a replacement for Si or WBG semiconductors. However, as compared to current WBG devices, it is not expected that β-Ga_2O_3 would enable more advanced converter topologies, and so benefits are likely to be incremental.

In contrast, at MV voltage levels (typically 1 kV to 33 kV for power distribution, or 2 kV to 15 kV for drives [35]) there is potential for high voltage β-Ga_2O_3 devices to enable greatly simplified converter topologies in high power AC drives and emerging MVDC applications. For example, the maximum voltage across a DC link V_{DC}^{Max} of an n-level VSC is typically limited to a fraction k of n times the voltage rating of the converters connected in series V_{Rated}, i.e.,

$$V_{DC}^{Max} = k \times n \times V_{Rated} \tag{1}$$

where the safety factor k could be 2/3 for simple two-level converters (i.e., a safety rating of around 50%) [36]. For example, six three-level neutral-point-clamped converters, with an AC-side line voltage of 2.1 kV and DC-side voltage of 4.5 kV, are combined to achieve a DC voltage of 27 kV in the MVDC ANGLE-DC demonstrator project [37]. If the voltage rating of β-Ga_2O_3 devices could be six times that of the Si IGBTs, the DC link voltage could be met with just a single three-level NPC converters. This is a substantial reduction in complexity as compared to the existing converters–e.g., each converter requires an additional winding on a bespoke transformer.

In AC drive applications, WBG devices are an enabling technology for high performance applications, typically using either SiC MOSFETs or GaN HEMTs [38]. For example, 3.3 kV SiC MOSFETs have been used to develop high performance MV Drives [39]. The cost, efficiency and topological flexibility enabled by β-Ga_2O_3 therefore has significant potential in this field of MV power converters.

For transmission system applications, IGBTs or thyristor devices are typically used, as they have much higher current and voltage ratings. Thyristors have been used for many decades in line commutated converter (LCC)-based HVDC, and continue to be an economical approach for GW-scale interconnection projects, such as the U.K.'s 2.2 GW Western Link [40]. Thyristors have the highest current and voltage ratings of the power semiconductor devices used in industry,

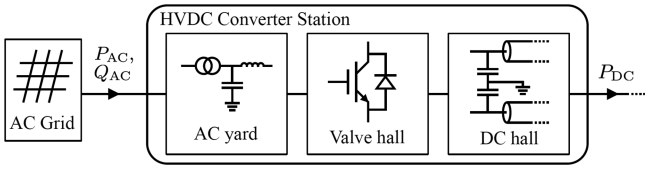

FIGURE 4. HVDC converter station topology.

and therefore could therefore be a potential application for β-Ga_2O_3. Similarly, VSC-based HVDC uses IGBT converters connected in series via an MMC topology to achieve high DC voltage and power levels. As with MV applications, the increased voltage rating can lead to a topology with fewer elements in series. Furthermore, the losses incurred in HVDC converter stations are known to be a substantial fraction of the overall system costs [41], and a growing number of offshore applications requiring high volumetric and a gravimetric density. Therefore, as the topology and efficiency of the converter is crucial, VSC-based HVDC can also seen as a significant potential application for β-Ga_2O_3 devices.

Flexible AC Transmission System (FACTS) equipment is a distinct family of transmission-connected devices that aim to increase utilization and controllability of transmission systems, and use a range of devices and energy storage elements to create shunt, series, or series-shunt FACTS devices that can inject voltages and currents [42]. The market uptake is modest, but there are examples of these technologies being applied to address issues resulting from power quality or dynamic response. For example, a 70 MVA static compensator (STATCOM) has been developed in the U.K. for transient response following network disturbances, using an MMC-based design using Si IGBT device [43]. MMC-based FACTS devices are would yield the same benefits as MMC-based HVDC systems.

B. β-GA_2O_3 FOR MMC-BASED VSCS

From the review in Section III-A, it can be concluded that β-Ga_2O_3 devices are of most interest in MV and HV applications, due to the flexibility that can be afforded in the converter topology, and, in high-performance converters requiring very low losses. VSC-HVDC is one of these topologies, and has a fast-growing market as compared to conventional LCC-based HVDC [44], and so has been selected to consider in more detail using the common half-bridge submodule topology. As compared to general MV converter applications, this topology has wide industry adoption; modellings in Section IV are closely related to a broad range of real implementations.

The main components of a HVDC converter station are shown in Fig. 4. The AC grid, typically at several hundred kV, can inject or draw real power P_{AC} and reactive power Q_{AC} from the converter station. The converter station first contains an AC yard, which can contain interfacing transformers, filters, and any necessary switchgear or auxiliary systems. A valve hall contains the half-bridge modules that together form the converters that transform power from AC to DC. The output of the valve hall is connected to a DC hall which may contain DC filters or any further auxiliary systems, before the power is transferred into the DC cable for transmission.

For a bipolar HVDC system, six valves will be constructed for three ac phases (one for positive and negative polarity), with each phase comprised of the required number of series connected submodules required to block the total DC voltage in the OFF-state. The number of series-connected submodules per valve is typically limited by the high DC voltage that must be blocked, with typical line-to line voltage of $\pm$320 kV needs to be shared between submodules. As a result, there are typically hundreds of series connected submodules. This has advantages of a reduction in filter requirements, with 100 units typically considered a sufficient number to avoid the requirement for an output filter altogether. In contrast, this large number of submodules leads to the need for a complex, high bandwidth control system and a high level of submodule redundancy for a given level of reliability, although higher operating voltages for each submodule device requires increased ratings of submodule auxiliaries, such as busbars and capacitors.

The β-Ga_2O_3's lower losses lead to a reduction in heat generation that must be dissipated by the thermal management system, a significant consideration in VSC-HVDC module design [40]. Reduced β-Ga_2O_3 losses also reduce \$-value of operating the system by reduction of the heat generation, and the need for a smaller cooling system. In challenging or constrained environments, such as offshore platforms, volumetric and gravimetric density are likely to be critical performance criteria, therefore making β-Ga_2O_3 particularly attractive.

IV. UWBG DEVICES IN MV/HV-DC CONVERTERS

To evaluate the effectiveness of different generation of β-Ga_2O_3 devices, as of β-Ga_2O_3/diamond and NiO_X/β-Ga_2O_3 in a grid-level application, we have modelled their benefit in the testbed of a half bridge MMC topology shown in Fig. 5. The device parameters are listed in Table 1 and system level parameters of the testbed are listed in Table 2, enabling analysis of the performance of commercially available 1.7 kV Silicon IGBT module by ABB with datasheet 5SNE 0800M170100 and 1.7 kV SiC power MOSFET module by Wolfspeed with datasheet CAS300M17BM2 compared with the state-of-the-art β-Ga_2O_3 power devices, including the laboratory prototypes of β-Ga_2O_3/diamond and NiO_X/β-Ga_2O_3 as in Table 1.

The β-Ga_2O_3 devices under evaluation range from early bulk β-Ga_2O_3 device with experimental results [45], [46] to the more recent ones demonstrated NiO_X/β-Ga_2O_3 [19], [47] together with the recent and latest experimental results of Gallium Oxide on diamond [19], [47], followed by analysis of theoretical potentials of β-Ga_2O_3/diamond in superjunction structures [29], [48], as listed in Table 1.

Two systems are selected for the study. The first is a 6 kV MVDC converter with power rating limited to 650 kW to understand the scope of the performance of these devices at distribution-level converters. The second is the MMC-VSC converter for HVDC transmission systems, rated at 320 kV

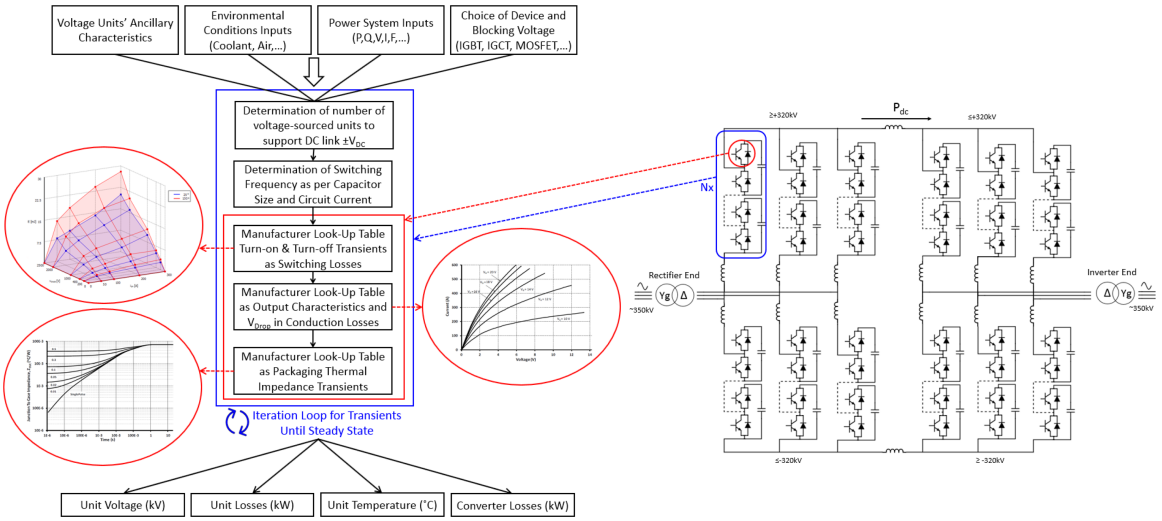

FIGURE 5. HVDC-VSC-MMC-HB converter topology is used as principal architecture to explore impact of device technology.

TABLE 1. Performance of Gallium Oxide Devices Compared to Similarly-Rated SiC Counterparts as Baseline as Per Literature [9], [19], [29], [45], [46], [47], [48], [49].

β-Ga_2O_3 Device Generation	R_{ON}	E_{SW}	R_{th}
β-Ga_2O_3 Experimental (2017-19)	5× [45], [47]	5× [46], [47]	10× [9]
NiO_X/β-Ga_2O_3 Experimental (2022)	0.2× [19]	3× [47]	10× [9]
NiO_X/β-Ga_2O_3 Experimental if grown on diamond substrate.	0.2× [19]	3× [47]	0.1*×
NiO_X/β-Ga_2O_3 Theoretical if grown on diamond substrate.	0.1× [20]	0.3× [49]	0.1*×
β-Ga_2O_3/diamond SJ Theoretical (2021)	0.1× [29]	0.02× [48]	0.1*×

* In this case, thermal resistance is determined by thickness of β-Ga_2O_3 layer. The relative thermal resistance of 0.1 with respect to SiC is obtained by assuming β-Ga_2O_3 is epitaxially grown on diamond. The thickness of epitaxial region is considered 100 times thinner than in bulk β-Ga_2O_3 devices. This thin epitaxially grown β-Ga_2O_3 in β-Ga_2O_3/diamond is expected to give 100x lower thermal resistance, i.e. 10/100=0.1.

TABLE 2. System-Level Parameters in the Models of the MVDC and VSC-HVDC converters [36], [37], [40], [44].

Case	Mode	V_{DC} (kV)	V_{AC} (kV)	I_{AC} (A)	P (MW)
1	MVDC Inv.	6	6.3	33	0.65
2	MVDC Rec.	6	6.3	33	0.65
3	HVDC Inv.	320	360	500	225
4	HVDC Rec.	320	360	400	200

TABLE 3. Converter-Level Parameters in the Models of the MVDC and VSC-HVDC converters [36], [37], [40], [44].

Parameter	MVDC Inv	MVDC Rec	HVDC Inv	HVDC Rec
Voltage per Module	1.2 kV	1.2 kV	1.2 kV	1.2 kV
Modules No.	12	12	600	600
Modules Utl.	83%	83%	89%	80%
Switching Freq.	198 Hz	192 Hz	50 Hz	72 Hz

with power ratings of 225 MW to analyse their performance as transmission-level converters. The list of the system-level properties are shown in Table 2.

As shown in the converter-level properties in Table 3, all modules are rated at 1700 V with voltage present on them derated to 1200 V. In the case of the MVDC converter, 12 modules are assumed in-circuit, while in the case of the VSC converter 600 modules are assumed to be in-circuit. To derive the power loss outputs, first the system conditions in Table 2 are considered by the developed model and accordingly the parameters in Table 3 are calculated to determine the utilisation factor and the switching frequency of the modules. The switching frequencies determined are sub-200 Hz which is in-line with the expectations [50], [51], [52], [53]. Following this, the time periods of on-state and number of switching transients are determined.

In the rectifier mode of operation, most of conduction is through the power diodes, although the switchings are still performed by the transistors. In the inverter mode of operation, most of conduction is through the power transistors, although the diodes are also conducting in dead-times. This means in the rectifier mode the power losses calculated are primarily dominated by the diodes, while in the inverter mode the power losses calculated are primarily dominated by the

transistors. The voltage rating of the submodule will ultimately determine the number of submodules needed to block a given DC voltage, i.e. the number of units needs increasing as the voltage rating of each unit decreases. The losses of the converter are calculated solely according to the information extracted from the datasheets for Si and SiC devices or as per Table 1. The following steps are used in modelling the conversion losses of the converter as described in [54], [55], [56], [57], [58]:

- The operating mode of the converter determined by the control algorithm is used to determine the load current through the transistor and anti-parallel diode in each valve, which can be calculated as:

$$I_P(t) = \frac{I_d}{3} + \frac{I_L \cdot \sqrt{2}}{2} sin(\omega t)$$
$$I_N(t) = \frac{I_d}{3} - \frac{I_L \cdot \sqrt{2}}{2} sin(\omega t) \quad (2)$$

  in which I_D is DC current, and I_L is the AC current.
- The recommended gate drive voltage is used to determine the ON-state voltage drop from the output characteristics. Here, a typical value of 15 V is considered in the look-ups of all datasheets.
- The temperature and current dependent conduction loss of the two transistors (T1, T2) and two diodes (D1, D2) in half-bridge are derived from a look-up table of losses which can be calculated as:

$$P_{T1}(t) = I_N(t) \cdot D \cdot V_{DS}(I_N, T)$$
$$P_{T2}(t) = I_P(t) \cdot (1 - D) \cdot V_{DS}(I_P, T)$$
$$P_{D1}(t) = I_P(t) \cdot D \cdot V_F(I_P, T)$$
$$P_{D2}(t) = I_N(t) \cdot (1 - D) \cdot V_F(I_N, T) \quad (3)$$

  Where N_M is number of modules, V_{ave} is voltage per module and V_{valve} is the total voltage, enabling calculation of D as:

$$D = \frac{V_{valve}(t)}{N_M \cdot V_{ave}(t)} \quad (4)$$

- The temperature and current dependent switching loss is calculated from a look-up table of losses which can be calculated as:

$$P_{SW} = f_{SW} \cdot (E_{on} + E_{off} + E_{rec}) \quad (5)$$

  in which, each of the turn-on, turn-off, and recovery energy can be calculated as:

$$E_{ON}, E_{OFF}, E_{RR} = \frac{T_j}{T_{Datasheet}} \cdot \frac{V_{DC}}{V_{Datasheet}} \cdot fitting(E_{datasheet}, K, I_d) \quad (6)$$

  in which K is the extrapolation factor for switching energy at different current levels based on second-order polynomial, described as [56], [57], [58]:

$$K = aI_d^2 + bI_d + c \quad (7)$$

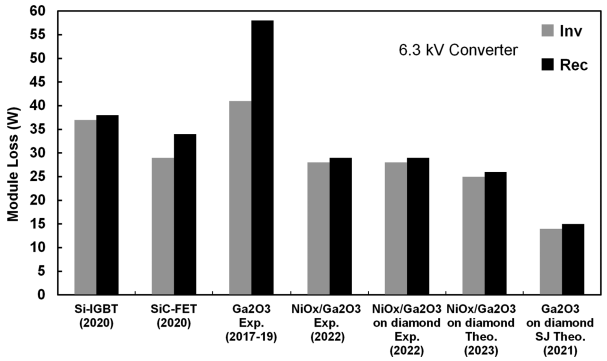

FIGURE 6. Power losses in the β-Ga_2O_3 modules in Table 1 compared with similarly-rated SiC-FET and Si-IGBT in the context of a 6.3 kV MVDC converter as in Tables 2 and 3.

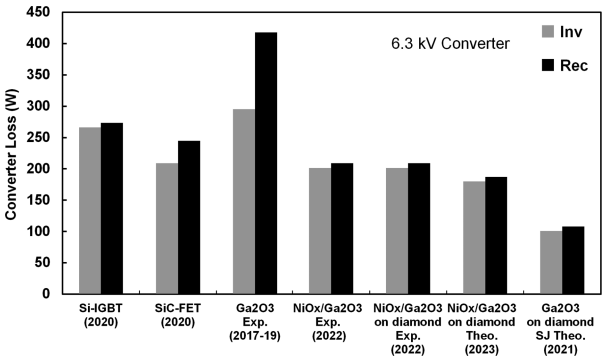

FIGURE 7. Power losses in the 6.3 kV MVDC converter as in Tables 2 and 3 when the β-Ga_2O_3 modules in Table 1 are implemented compared with similarly-rated SiC-FET and Si-IGBT.

- The combined losses are input to a thermal model which is derived from the datasheet thermal impedance characteristics (the ambient temperature is fixed at coolant temperature) as

$$\Delta T = T_j - T_a = P_{Total} \cdot R_{th-j-a} \quad (8)$$

- The calculated temperature (T_j) is used to determine increased losses together with the load current and switching state, which defines the Temperature in (3) and (6) for the conduction and switching losses, respectively.

The results of the two converters analysed are discussed in the following:

A. DISTRIBUTION-LEVEL MEDIUM VOLTAGE DC (MVDC) CONVERTER:

As can be seen in Fig. 6, the power losses at module level when considering the use of early experimental β-Ga_2O_3 devices (2017-2019) are higher compared to when using Si-IGBTs and SiC-FETs, though this difference reduces once the potential of β-Ga_2O_3/diamond superjunctions are considered (2022-onwards). The per-unit of total converter losses compared with the overall system power is considerable, which can be seen in Fig. 7. Here, the losses of the individual modules have shaped the total losses in the converter, which

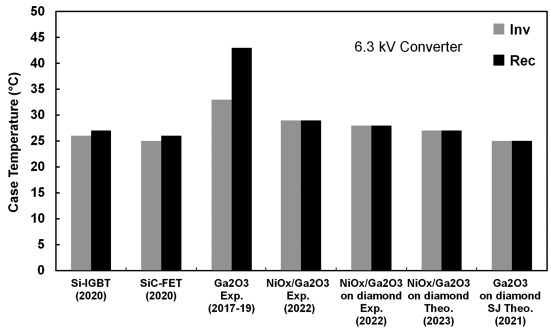

FIGURE 8. Module case temperature in the β-Ga_2O_3 modules in Table 1 compared with similarly-rated SiC-FET and Si-IGBT in the context of a 6.3 kV MVDC converter as in Tables 2 and 3.

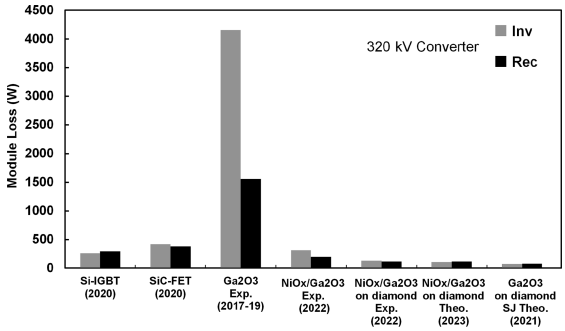

FIGURE 9. Power losses in the β-Ga_2O_3 modules in Table 1 compared with similarly-rated SiC-FET and Si-IGBT in the context of a 320 kV MMC-VSC-HVDC converter as in Tables 2 and 3.

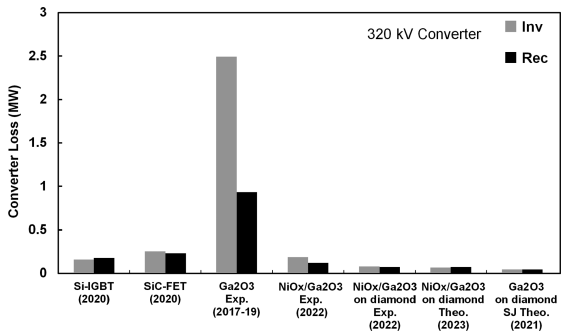

FIGURE 10. Power losses in the 320 kV VSC-HVDC converter as in Tables 2 and 3 when the β-Ga_2O_3 modules in Table 1 are implemented compared with similarly-rated SiC-FET and Si-IGBT.

follows the same trend of Fig. 6 as expected. These are for β-Ga_2O_3 modules with different technologies as per Table 1. It can be seen that the losses decrease from early β-Ga_2O_3 devices (2017–2019) to less than half if the theoretical potential of β-Ga_2O_3/diamond superjunctions are realized, which is lower than when using a Si or SiC device; even current experimentally realized β-Ga_2O_3 devices provide improvements compared to Si and SiC devices. The per-unit level of the module losses could be reduced even further by moving toward NiO_X-β-Ga_2O_3/diamond substrates. The MVDC converters are likely to be more abundantly available on the distribution-level energy networks compared with HVDC transmission lines. The distribution systems infrastructure is an order of magnitude more extensive than transmission systems in terms of length of overhead lines and cables [59],so these losses can add up to a significant value, making the case to move toward the more efficient NiO_X-β-Ga_2O_3/diamond substrates.

The impact of power losses on increased case temperature of the modules is shown in Fig. 8 which shows a temperature rise observed in the bulk β-Ga_2O_3 devices (2017–2019) compared with the other devices; the losses in Fig. 6 do not lead to a significant temperature rise in this case, given the substantial cooling system that is assumed available on the case of the modules. The temperature rise is more significant in early bulk β-Ga_2O_3 devices, though it is less evident in later generations of β-Ga_2O_3 devices due to the low absolute value of the power losses in the system. The rise of case temperature will be more clearly visible when power losses per module increase, the case in more powerful transmission HVDC systems to be discussed next.

B. TRANSMISSION-LEVEL VOLTAGE-SOURCED HVDC CONVERTER:

We evaluated the impact of using β-Ga_2O_3 for a heavy-duty 320 kV, 225 MW converter in the context of a MMC-VSC-HVDC converter. It is evident that the performance when using early generation of β-Ga_2O_3 devices (2017–2019), as per the experimental results [9], would be rather poor compared to the state-of-the-art Si-IGBT and SiC-FETs, as evident in Fig. 9. Considering the more recent experimental results of the bulk β-Ga_2O_3 devices (2023), their use reduces the converter losses which starts to deliver advantages for using β-Ga_2O_3 modules compared with the Si-IGBT and SiC-FETs. The issue of the thermal conductivity is resolved in the latest results of experiments on the β-Ga_2O_3 grown on diamond substrates indicating significantly improved thermal properties [26]. This, coupled with the superior performance of the β-Ga_2O_3/diamond devices in terms of on-state resistance and switching losses has led to significantly lower power losses in modules (by up to a third compared to incumbent Si-IGBT and SiC-FETs) as is attested by Fig. 9. This, given that the device properties are experimental data, and even though devices are fabricated in research laboratories rather than industrially, is very promising. It is noteworthy that the SiC-FET module in this context is actually performing worse than the Si-IGBT module, given the low switching frequency and long on-state periods which gives an edge to the slow IGBTs which take advantage of conductivity modulation to reduce the on-state losses. Although superjunction structure of β-Ga_2O_3/diamond devices have not been yet fabricated, theoretical analysis by computer-aided designs indicate that should these devices be developed, they will enable even further reduction in power losses in modules, with the impact on losses also depicted in Fig. 9, compared to the latest β-Ga_2O_3/diamond devices demonstrated experimentally.

Fig. 10 indicates the trends of total power losses in the context of the heavy-duty MMC-VSC-HVDC converter application. It can be seen that the early generation of β-Ga_2O_3

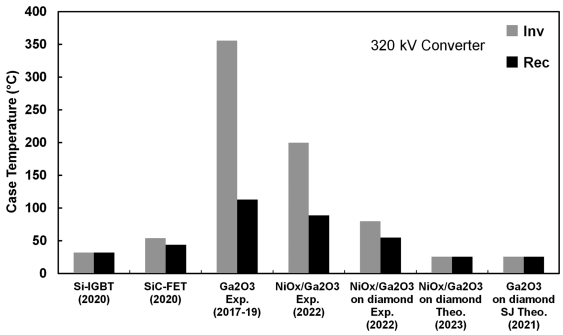

FIGURE 11. Module case temperature in the β-Ga_2O_3 modules in Table 1 compared with similarly-rated SiC-FET and Si-IGBT in the context of a 320 kV MMC-VSC-HVDC converter as in Tables 2 and 3.

devices (2017–2019) deliver a poor performance overall, as was expected from the individual modules' losses. However, the latest developments by of heterogenous integration of β-Ga_2O_3 with diamond with substrate thinning have significantly improved their performance metrics, especially in terms of thermal management. The theoretical potential of the device indicate even better performance is achievable, which could be materialized experimentally in foreseeable future.

The same trends are observed in Fig. 11 in terms of case temperature rise of the devices. The higher losses in early generation of β-Ga_2O_3 devices are also reflected in an increased case temperature with temperatures in excess of 350°C when the converter is primarily operating by switching the transistors in the inverter mode as in Fig. 11. Device temperature are sub-optimal, given the low thermal conductivity of first generation β-Ga_2O_3 modules fabricated in 2017–2019. The case temperatures is adequately lowered though when moving to the recent generations of β-Ga_2O_3/NiO_X on diamond substrates as in Fig. 11 thanks to the reduced thermal resistance by substrate thinning on diamond.

V. CONCLUSION

This work evaluated the performance of several generations of β-Ga_2O_3 devices in the context of heavy-duty MMC-based VSC converters compared with the incumbent Si-IGBTs & SiC-FETs for HVDC and MVDC converter station applications. A range of potential applications for β-Ga_2O_3 devices were considered, with MMC-VSC selected for detailed study as a converter topology with both wide industry uptake and significant potential to exploit β-Ga_2O_3 devices' high voltage and high efficiency operation. It is shown that the recently demonstrated β-Ga_2O_3 devices could make a significant difference to the performance of both MVDC & HVDC power converters in grid-level applications with comparable efficiency gains, in particular when the latest generation of β-Ga_2O_3 devices are implemented. The results show that although the early bulk β-Ga_2O_3 devices fabricated and measured in research laboratories would perform poorly, this changes when the device is fabricated as NiO_X/β-Ga_2O_3 and on diamond substrate, leading to a significantly lower thermal resistance which in turn reduces the power dissipation. The β-Ga_2O_3/diamond devices can outperform the incumbent Silicon and SiC devices in terms of individual module performance dramatically, leading to reduced losses at the converter, with reduced elevations in the case temperatures. This can be further enhanced should the β-Ga_2O_3/diamond is fabricated in superjunction structures in foreseeable future, or other advanced device concepts.

ACKNOWLEDGMENT

All underlying data for this article are provided within, or in the cited references.

REFERENCES

[1] F. Umbach et al., "2.3 kV–A new voltage class for Si IGBT and Si FWD," in *Proc. IEEE Int. Exhib. Conf. Power Electron., Intell. Motion, Renewable Energy Energy Manage.*, 2020, pp. 1–7.
[2] J. Rabkowski, D. Peftitsis, and H. -P. Nee, "Silicon carbide power transistors: A new era in power electronics is initiated," *IEEE Ind. Electron. Mag.*, vol. 6, no. 2, pp. 17–26, Jun. 2012.
[3] H. Amano et al., "The 2018 GAN power electronics roadmap," *J. Phys. D: Appl. Phys.*, vol. 51, 2018, Art. no. 163001.
[4] Y. Gunaydin, "Analysis of performance and reliability of sub-kV SiC and GAN cascode power electronic devices," Ph.D. dissertation, Univ. Bristol, Bristol, U.K., 2023, doi: 10.13140/RG.2.2.20071.62882.
[5] S. Jahdi, O. Alatise, J. O. Gonzalez, L. Ran, and P. Mawby, "Comparative analysis of false turn-on in silicon bipolar and SiC unipolar power devices," in *Proc. IEEE Energy Convers. Congr. Expo.* 2015, pp. 2239–2246.
[6] J. Yang, S. Jahdi, B. Stark, R. Wu, O. Alatise, and J. O. Gonzalez, "Impact of temperature and switching rate on properties of crosstalk on symmetrical & asymmetrical double-trench SiC power MOSFET," in *Proc. IEEE 47th Annu. Conf. Ind. Electron. Soc.*, 2021, pp. 1–6.
[7] S. Jahdi, O. Alatise, J. A. Ortiz Gonzalez, R. Bonyadi, L. Ran, and P. Mawby, "Temperature and switching rate dependence of crosstalk in Si-IGBT and sic power modules," *IEEE Trans. Ind. Electron.*, vol. 63, no. 2, pp. 849–863, Feb. 2016.
[8] B. J. Baliga, "Semiconductors for high-voltage, vertical channel field-effect transistors," *J. Appl. Phys.*, vol. 53, no. 3, pp. 1759–1764, 1982.
[9] M. Higashiwaki, "β-gallium oxide devices: Progress and outlook," *Physica Status Solidi (RRL) – Rapid Res. Lett.*, vol. 15, no. 11, 2021, Art. no. 2100357.
[10] S. Reese et al., "How much will gallium oxide power electronics cost?," *Joule*, vol. 3, no. 4, pp. 903–907, 2019.
[11] M. Higashiwaki et al., "Gallium oxide (Ga2O3) metal-semiconductor field-effect transistors on single-crystal β-Ga2O3 (010) substrates," *Appl. Phys. Lett.*, vol. 100, no. 1, 2012, Art. no. 013504.
[12] M. Higashiwaki et al., "Temperature-dependent capacitance–voltage and current–voltage characteristics of Pt/Ga2O3 (001) Schottky barrier diodes fabricated on n-–Ga2O3 drift layers grown by halide vapor phase epitaxy," *Appl. Phys. Lett.*, vol. 108, no. 13, 2016, Art. no. 133503.
[13] K. Konishi et al., "1-kV vertical Ga2O3 field-plated Schottky barrier diodes," *Appl. Phys. Lett.*, vol. 110, no. 10, 2017, Art. no. 103506.
[14] C.-H. Lin et al., "Vertical Ga2O3 Schottky barrier diodes with guard ring formed by nitrogen-ion implantation," *IEEE Electron Device Lett.*, vol. 40, no. 9, pp. 1487–1490, Sep. 2019.
[15] W. Li et al., "2.44 kV Ga2O3 vertical trench Schottky barrier diodes with very low reverse leakage current," in *Proc. IEEE Int. Electron Devices Meeting*, 2018, pp. 8.5.1–8.5.4.
[16] W. Li et al., "Fin-channel orientation dependence of forward conduction in kV-class Ga2O3 trench Schottky barrier diodes," *Appl. Phys. Exp.*, vol. 12, no. 6, May 2019, Art. no. 061007.
[17] T. Watahiki et al., "Heterojunction p-Cu2O/n-Ga2O3 diode with high breakdown voltage," *Appl. Phys. Lett.*, vol. 111, no. 22, 2017, Art. no. 222104.
[18] Y. Wang et al., "2.41 kV vertical p-Nio/n-Ga2O3 heterojunction diodes with a record Baliga's figure-of-merit of 5.18 GW/cm2," *IEEE Trans. Power Electron.*, vol. 37, no. 4, pp. 3743–3746, Apr. 2022.
[19] J. Zhang et al., "Ultra-wide bandgap semiconductor Ga2O3 power diodes," *Nature Commun.*, vol. 13, 2022, Art. no. 3900.

[20] J.-S. Li et al., "Reproducible Nio/Ga2O3 vertical rectifiers with breakdown voltage >8 kV," *Crystals*, vol. 13, 2023, Art. no. 886.
[21] R. Sharma et al., "Effect of probe geometry during measurement of >100 a Ga2O3 vertical rectifiers," *J. Vac. Sci. Technol. A*, vol. 39, no. 1, 2021, Art. no. 013406 .
[22] M. Singh et al., "Pulsed large signal RF performance of field-plated Ga2O3 MOSFETs," *IEEE Electron Device Lett.*, vol. 39, no. 10, pp. 1572–1575, Oct. 2018.
[23] N. Moser et al., "Toward high voltage radio frequency devices in β-Ga2O3," *Appl. Phys. Lett.*, vol. 117, no. 24, 2020, Art. no. 242101.
[24] T. Moule et al., "Breakdown mechanisms in β-Ga2O3 trench-MOS Schottky-barrier diodes," *IEEE Trans. Electron Devices*, vol. 69, no. 1, pp. 75–81, Jan. 2022.
[25] Y. Qin et al., "Thermal management and packaging of wide and ultra-wide bandgap power devices: A review and perspective," *J. Phys. D: Appl. Phys.*, vol. 56, 2023, Art. no. 093001.
[26] Z. Cheng et al., "Integration of polycrystalline Ga2O3 on diamond for thermal management," *Appl. Phys. Lett.*, vol. 116, no. 6, 2020, Art. no. 062105.
[27] P. Sittimart et al., "Diamond/β-Ga2O3 pn heterojunction diodes fabricated by low-temperature direct-bond," *AIP Adv.*, vol. 11, 2021, Art. no. 105114.
[28] S. H. Kim et al., "Transient thermal management of a β-Ga2O3 MOSFET using a double-side diamond cooling approach," *IEEE Trans. Electron Devices*, vol. 70, no. 4, pp. 1628–1635, Apr. 2023.
[29] A. Mishra, Z. Abdallah, J. W. Pomeroy, M. J. Uren, and M. Kuball, "Electrical and thermal performance of Ga2O3–Al2O3–diamond superjunction Schottky barrier diodes," *IEEE Trans. Electron Devices*, vol. 68, no. 10, pp. 5055–5061, Oct. 2021.
[30] S. R. Bench Reese, K. A. Horowitz, T. W. Remo, M. K. Mann, and J. Cresko, "A techno-economic look at SiC WBG from wafer to motor drive," *Nat. Renewable Energy Lab.*, Golden, CO, USA, Tech. Rep. NREL/PR-6A20-71240, 2018.
[31] E. Kabalci, "Review on novel single-phase grid-connected solar inverters: Circuits and control methods," *Sol. Energy*, vol. 198, pp. 247–274, 2020.
[32] Y. Yang et al., "Tesla and silicon carbide: Optimistic outlook overrides initial panic," 2023. Accessed: Aug. 17, 2023. [Online]. Available: https://www.yolegroup.com/strategy-insights/tesla-and-silicon-carbide-optimistic-outlook-overrides-initial-panic/
[33] U.K. Power, "Engineering operating standard eos 09-0042: Fun-lv multi-terminal power electronics devices," 2015. Accessed: Aug. 17, 2023. [Online]. Available: https://innovation.ukpowernetworks.co.uk/projects/fun-lv/
[34] U.K. Power, "Active response to distribution network constraints–network innovation competition 2017 submission," 2017. Accessed: Aug. 17, 2023. [Online]. Available: https://innovation.ukpowernetworks.co.UK/wp-content/uploads/2018/12/Active-Response-FSP.pdf
[35] K. Horowitz et al., "A manufacturing cost and supply chain analysis of SiC power electronics applicable to medium-voltage motor drives," *Nat. Renewable Energy Lab.*, Golden, CO, USA, Tech. Rep. NREL/TP-6A20-67694, 2017. [Online]. Available: www.osti.gov/biblio/1349212
[36] Backlund and Carroll, "Voltage ratings of high power semiconductors," 2006. Accessed: Aug. 17, 2023. [Online]. Available: https://5scomponents.com/pdf/voltage_ratings_of_high_power_semiconductors.pdf
[37] SP Energy Networks, "Angle-DC: Close down report," 2022. Accessed: Aug. 17, 2023. [Online]. Available: www.spenergynetworks.co.uk/userfiles/file/Angle-DC_Close_Down_Report.pdf
[38] A. K. Morya et al., "Wide bandgap devices in AC electric drives: Opportunities and challenges," *IEEE Trans. Transport. Electrific.*, vol. 5, no. 1, pp. 3–20, Mar. 2019.
[39] A. Marzoughi, R. Burgos, and D. Boroyevich, "Investigating impact of emerging medium-voltage SiC MOSFETs on medium-voltage high-power industrial motor drives," *IEEE Trans. Emerg. Sel. Topics Power Electron.*, vol. 7, no. 2, pp. 1371–1387, Jun. 2019.
[40] Siemens, "HVDC classic–powerful and economical," 2021. Accessed: Aug. 17, 2023. [Online]. Available: https://assets.siemens-energy.com/siemens/assets/api/uuid:8572c795-95c7-49e 8-8367-dc578b4e59a5/2021-09-27-hvdc-classic.pdf
[41] D. Van Hertem et al., "Comparison of HVAC and HVDC technologies," in *HVDC Grids: For Offshore and Supergrid of the Future*. Hoboken, NJ, USA: Wiley, 2016, pp. 79–96.
[42] N. G. Hingorani and L. Gyugyi, *FACTS Concept and General System Considerations*. Hoboken, NJ, USA: Wiley, 1999.
[43] SP Energy Networks, "Phoenix–system security and synchronous condenser," 2017. Accessed: Aug. 17, 2023. [Online]. Available: www.spenergynetworks.co.uk/userfiles/file/Phoenix_Progress_Report_Dec_2017.pdf
[44] Nishioka et al., "Global rise of HVDC and its background," 2020. Accessed: Aug. 17, 2023. [Online]. Available: www-origin.hitachi.com/rev/archive/2020/r2020_04/pdf/gir.pdf
[45] N. Allen et al., "Vertical Ga2O3 Schottky barrier diodes with small-angle beveled field plates: Baliga's figure-of-merit of 0.6 GW/cm2," *IEEE Electron Device Let.*, vol. 40, no. 9, pp. 1399–1402, Sep. 2019.
[46] K. Chabak et al., "Recessed-gate enhancement-mode β-Ga2O3 MOSFETs," *IEEE Electron Device Lett.*, vol. 39, no. 1, pp. 67–70, Jan. 2018.
[47] F. Wilhelmi et al., "Switching properties of 600 V Ga2O3 diodes with different chip sizes and thicknesses," *IEEE Trans. Power Electron.*, vol. 38, no. 7, pp. 8406–8418, Jul. 2023.
[48] M. Kong et al., "A novel Ga2O3 superjunction LDMOS using P-Type diamond with improved performance," *ECS J. Solid State Sci. Technol.*, vol. 11, no. 10, 2022, Art. no. 105006.
[49] G. Jessen et al., "Gallium oxide technologies and applications," in *Proc. IEEE Compound Semicond. Integr. Circuit Symp.*, 2017, pp. 1–4.
[50] A. Hassanpoor et al., "Loss evaluation for modular multilevel converters with different switching strategies," in *Proc. IEEE 9th Int. Conf. Power Electron. ECCE Asia*, 2015, pp. 1558–1563.
[51] Q. Tu, Z. Xu, and L. Xu, "Reduced switching-frequency modulation and circulating current suppression for modular multilevel converters," *IEEE Trans. Power Del.*, vol. 26, no. 3, pp. 2009–2017, Jul. 2011.
[52] A. Nami, J. Liang, F. Dijkhuizen, and G. D. Demetriades, "Modular multilevel converters for HVDC applications: Review on converter cells and functionalities," *IEEE Trans. Power Electron.*, vol. 30, no. 1, pp. 18–36, Jan. 2015.
[53] A. António-Ferreira et al., "Modular multilevel converter losses model for HVDC applications," *Elect. Power Syst. Res.*, vol. 146, pp. 80–94, 2017.
[54] *Amendment 2 - Power Losses in Voltage Sourced Converter (VSC) Valves for High-Voltage Direct Current (HVDC) Systems - Part 2: Modular Multilevel Converters*, IEC Standard 62751-2:2014/AMD2:2023, Aug. 2023.
[55] P. A. Gbadega and A. K. Saha, "Loss assessment of MMC-based VSC-HVDC converters using IEC 62751-1-2 Standard and component datasheet parameters," in *Proc. IEEE PES/IAS PowerAfrica*, 2018, pp. 1–9.
[56] C. Xu et al., "Power loss analysis of a novel modular multilevel converter based on semi-full-bridge sub-module with SiC-MOSFET switched capacitors," in *Proc. 1st Workshop Wide Bandgap Power Devices Appl. Asia*, 2018, pp. 45–54.
[57] Z. Zhang, Z. Xu, and Y. Xue, "Valve losses evaluation based on piecewise analytical method for MMC–HVDC links," *IEEE Trans. Power Del.*, vol. 29, no. 3, pp. 1354–1362, Jun. 2014.
[58] V. Kartsonakis, "Semiconductors power losses in a three-phase inverter using matlab application designer," M.S. thesis, Sch. Eng. Sci., Aalborg Univ., Aalborg, Denmark, 2021.
[59] National Grid, "What's the difference between electricity transmission and distribution?," 2022. Accessed: Aug. 17, 2023. [Online]. Available: www.nationalgrid.com/stories/energy-explained/electricity-transmission-vs-electricity-distribution

SAEED JAHDI (Senior Member, IEEE) received the Ph.D. degree in power electronics from the University of Warwick in Coventry, Coventry, U.K., in 2016. He was with the HVDC Center of Excellence of General Electric, General Electric Grid Solutions, Stafford, U.K., as a Power Electronics Engineer and Line-Coordinator on several onshore and offshore VSC-HVDC projects in the U.K., Germany, Sweden, France, and Italy. He is currently an Assistant Professor of power electronics with the Electrical Energy Management Group, University of Bristol, Bristol, U.K. He is also a Chartered Engineer with the U.K. IET. His research focuses on wide-bandgap power semiconductor devices in power electronics. He was the recipient of the GE's competitive Early-Career Engineering Award in 2018 for contribution to the success of these flagship HVDC projects by GE and 2021 outstanding paper award for the IEEE Transactions on Industrial Electronics.

AKHIL S. KUMAR (Member, IEEE) received the B.Tech. degree from the India National Institute of Technology Karnataka, Mangalore, India, and the Ph.D. degree in fabrication, characterization, and modeling of III-V based HEMTs and nanowire transistors from the Indian Institute of Technology, Bombay, Mumbai, India. Since 2020, he has been a Postdoctoral Research Associate with the University of Bristol, Bristol, U.K. His research interests include reliability of multichannel GaN transistors for RF and switching applications.

MATTHEW DEAKIN (Member, IEEE) received the M.Eng. and D.Phil. (Ph.D.) degrees in engineering science from the University of Oxford, Oxford, U.K., in 2015 and 2020, respectively. He was the recipient of the Lubbock Prize for the M.Eng. degree and held a Clarendon Ph.D. Scholarship from the University of Oxford. He is currently a Royal Academy of Engineering Research Fellow with Newcastle University, Newcastle upon Tyne, U.K., where he was a Research Associate from 2019 to 2022. His research interests include distribution system analysis, hybrid AC/DC grids, and smart grids.

PHIL C. TAYLOR (Senior Member, IEEE) is currently the Pro Vice-Chancellor of Research and Enterprise with the University of Bristol, Bristol, U.K. He has worked in energy systems in industry and academia for more than 25 years. In 2013, he joined Newcastle University, Newcastle upon Tyne, U.K., as the Dean and the Director of the multidisciplinary Institute for Sustainability, and later, became the Head of the School of Engineering. He is the Director of the £10 M EPSRC Supergen Energy Networks Hub, which brings together industrial and academic partners including seven U.K. universities. His Industrial experiences include GEC Alstom, EPS, U.K., Teradyne, and Senergy Econnect. He is an independent Member of the U.K. Government's Net Zero Innovation Board and a Visiting Professor with Nanyang Technological University, Singapore. He is a nonexecutive Director of Northern Powergrid, an electrical distribution company, which provides power to eight million customers in the North East and Yorkshire. He is a Member of the Board of Trustees for National Energy Action, a fuel poverty charity.

MARTIN KUBALL (Fellow, IEEE) received the Ph.D. degree from the Max Planck Institute for Solid State Research, Stuttgart, Germany. He is Royal Academic of Engineering Chair in Emerging Technologies, and Director of the Innovation and Knowledge Centre REWIRE and Center for Device Thermography and Reliability, University of Bristol, Bristol, U.K. His research interests include wide and ultrawide bandgap semiconductor power and RF materials and device technologies. He was the recipient of the He Bong Kim Award in 2010 and Royal Society Wolfson Award in 2015. He is a Fellow of MRS, SPIE, IET, and IoP. He joined the University of Bristol in 1997 from Brown University, Providence, RI, USA.